

1 When should patch connectivity affect local species 2 richness? Pinpointing adequate methods in adequate 3 landscapes using simulations.

4 F. Laroche^{1*}, M. Balbi¹, T. Grébert², F. Jabot² & F. Archaux¹

5 ¹Irstea, UR EFNO, Domaine des Barres, F-45290 Nogent-sur-Vernisson, France

6 ²Université Clermont Auvergne, Irstea, UR LISC, Centre de Clermont-Ferrand, F-63178

7 Aubière, France

8 *corresponding author: fabien.laroche@irstea.fr

9 Abstract

10 The Theory of Island Biogeography (TIB) promoted the idea that species richness within
11 sites should depend on site connectivity, i.e. its connection with surrounding potential
12 sources of immigrants. TIB has been extended to a wide array of fragmented ecosystems,
13 beyond archipelagoes, surfing on the analogy between habitat patches and islands and the
14 patch-matrix framework. However, patch connectivity often little contributes to explaining
15 species richness in empirical studies. Before interpreting this trend as questioning the broad
16 applicability of TIB principles, one first needs a clear identification of methods and contexts
17 where strong effects of patch structural connectivity are likely to occur. Here, we use spatially
18 explicit simulations of neutral metacommunities to show that patch connectivity effect on
19 local species richness is maximized under a set of specific conditions: (i) patch delineation
20 should be fine enough to prevent dispersal limitation within patches, (ii) patch connectivity
21 indices should be scaled according to target organisms' dispersal abilities and (iii) habitat
22 amount and fragmentation should both lie in some intermediary range that still needs an
23 empirically tractable definition. When those three criteria are met, the absence of effect of
24 connectivity on species richness should be interpreted as contradicting TIB principles.

25 Key-words

26 Landscape ecology; Structural connectivity; Virtual ecologist; Neutral landscapes; Dispersal;
27 Diversity patterns; Habitat amount hypothesis

28 Introduction

29 Since the Theory of Island Biogeography (TIB) [1], it is commonly acknowledged that species
30 presence within local community depends on their ability to immigrate, and that geographic
31 isolation of communities can negatively affect species richness. TIB principles have been
32 extended to a wide array of ecosystems beyond archipelagoes (see [2,3] for reviews and
33 critical appraisal), leading to studying how the availability of suitable habitat nearby can act
34 as a source of immigrants and affect species richness within local communities. Such
35 generalization of TIB relied on adopting a “patch-matrix” description of habitat in space,
36 where one decomposes the map of some suitable habitat into patches that correspond to
37 potential communities (analogous to islands in an archipelago), the rest of space being
38 considered inhospitable for species.

39 The geographic isolation of patches has been developed into the concept of “patch structural
40 connectivity”, which quantifies the potential exchanges of immigrants between a focal patch
41 and the surrounding habitats [4]. Most of the indices that aim at quantifying patch structural
42 connectivity consist in counting patches around the focal patch, using weights proportional to
43 patch area (or quality) and decreasing with distance to the focal patch. For instance, the
44 “distance to nearest neighbor” index gives weight 1 to the closest patch and 0 for others.
45 Buffer indices give positive weights to patches closer to the focal patch than some threshold
46 distance, and weight 0 to patches outside this range. More generally, indices based on a
47 distance kernel give to patches weights that decrease with distance to the focal patch
48 according to some pre-defined kernel function (e.g. [5]).

49 In a meta-analysis of 1'015 empirical studies on terrestrial systems covering a broad
50 taxonomical range and spread at global scale, [6] evidenced that patch structural connectivity
51 measured as distance to the nearest patch tend to have weak predictive power on species
52 presence within patches (median deviance explained equaled c.a. 20%). This study brings
53 some evidence showing that the limited success of patch connectivity indices may come
54 from: inadequate use of structural connectivity indices based on surrounding habitat rather
55 than functional connectivity indices based on surrounding populations, inadequate
56 delineation of patches for species harboring multiple life stages with contrasted requirements
57 and overlooking the type of matrix surrounding the habitat patch, hence questioning the
58 validity of the patch-matrix framework for terrestrial systems.

59 Questioning the validity of the TIB or the patch-matrix framework for terrestrial systems or
60 arguing for the use of functional rather than structural patch connectivity indices are sound
61 criticism of current practices. However, the TIB framework based on structural connectivity is

62 has the strong advantage of being quite simple and straightforward to implement in a broad
63 array of empirical systems. Before discarding it for more involved methodologies, one should
64 make sure that its limited success in past studies does not come from methodological
65 limitations that can be fixed. For instance, another review of 122 empirical studies [7], which
66 covered terrestrial and aquatic systems and analyzed the presence or abundance of 954
67 species, evidenced that effects of local environmental conditions within a patch on species
68 presence or abundance occurred more frequently (71% of species analyses) than the effects
69 of patch structural connectivity (55% of species analyses). These authors mentioned
70 methodological limits as a major explanation of the limited success of patch structural
71 connectivity indices: the lack of statistical power, i.e. insufficient number of patches and the
72 inadequate patch structural connectivity metrics, buffer indices being more performant than
73 widely used isolation metrics. Here we argue that a critical appraisal of the TIB framework
74 needs identifying first which methods for measuring patch structural connectivity and which
75 properties of the habitat spatial distribution of studied systems are expected to yield strong
76 effects of patch structural connectivity on local species richness. If the TIB framework fails
77 when both methods and context are expected to be adequate then the conceptual ground of
78 the approach can be undoubtedly questioned.

79 The lack of strong effects of patch structural connectivity indices on local species richness
80 may come from the fact that the patch structural connectivity indices used in empirical
81 studies do not efficiently capture the immigration intensity. For instance, [8,9] showed that
82 indices based on the distance to the nearest patches are poor predictors of species presence
83 compared indices based on a distance kernel, like buffers. [9] further showed that even when
84 complementing distance to nearest patches with the area of the focal patch, buffer were still
85 better predictor of species richness. This tend to suggest that patch connectivity indices can
86 intrinsically differ in their ability to capture the contribution of immigration to species richness
87 within a focal patch. Here, we aimed at comparing how three types of patch connectivity
88 indices coming from contrasted frameworks differed or not in their explanatory power of
89 species richness.

90 Among indices based on a distance kernel, the tuning of “scaling parameters” (i.e.
91 parameters driving the speed of patch weight decrease with distance) with respect to target
92 organisms dispersal also modulates the explanatory power of patch connectivity indices.
93 Using simulations of a metacommunity on patch networks, [10] showed that changing the
94 scaling of patch connectivity indices (i.e. how fast patch weights decrease with distance) can
95 change the effect size of connectivity on species Simpson diversity. They further showed that
96 the higher the dispersal ability of species, the larger the scaling of indices should be to reach
97 the best possible explanatory power. Similarly, a metapopulation simulation study [11]

98 showed that there exists some optimal buffer radius that maximizes the effect size of
99 connectivity upon local presence of a target species. They further suggested that this optimal
100 size, called the “scale of effect” should lie between four and nine times the average dispersal
101 distance of the target species. Therefore, choosing an appropriate scaling of patch
102 connectivity indices with respect to typical dispersal distances of target organisms should
103 improve the ability of patch connectivity indices to capture a negative effect of geographic
104 isolation on species richness. Here, we aimed at testing whether the scaling of patch
105 connectivity indices that maximizes the explanatory power upon species richness increased
106 with dispersal distance of target organisms, as suggested by previous findings.

107 Patch definition and delineation must adapt to the questions and patterns under study [12].
108 For instance, in studies about foraging strategies, defining a patch according to the
109 perceptual range of target organisms can be adequate. By contrast, in the context of the TIB,
110 patches should correspond to discrete areas of habitat within which individuals from multiple
111 species have access and compete for all the resource without space limitation over their
112 lifetime, hence making relevant entities for community-scale studies. [12] extensively
113 developed how focusing on inappropriate patch scale in optimal foraging could lead to
114 unexpected patterns. Similarly, [13] showed in a simulation study that the negative
115 relationship between species richness and distance to mainland in the classic TIB may
116 collapse when applied to entire archipelagoes rather than single islands, because of internal
117 limited dispersal. Therefore, a decisive step in the analysis of patch connectivity effects on
118 local species richness is therefore to convert the raw raster of habitat pixels into patches of
119 appropriate size. Often, the delineation of patches follows a “vector map” perspective,
120 according to [14] terminology : set of contiguous pixels corresponding to “habitat” are lumped
121 together to form polygons denoted as patches. However, this approach brings no guarantee
122 that emerging patches have the appropriate size to constitute potential communities for
123 target organisms. In particular, when habitat is little fragmented, it creates large patches and
124 subsequent connectivity indices potentially miss a large part of connectivity effects, which
125 may take place within patches. Such mismatch may weaken the link between patch-based
126 connectivity and community features measured from a local sample. We propose that
127 building patches from a “raster” perspective (still following [14] terminology), using a grid with
128 mesh size smaller or equal to the average dispersal distance of target organisms should
129 ensure the appropriate patch delineation for the study and contribute to increase the
130 explanatory power of patch connectivity indices on species richness. In particular, large
131 contiguous sets of habitat pixels should be split to obtain patches of adequate dimension.
132 Here, we aimed at comparing the performance of patch connectivity indices computed from a
133 vector map perspective to those obtained from a raster perspective with mesh size adapted

134 to the dispersal distance of target organisms. We expected that using a raster with mesh size
135 smaller or equal to the dispersal distance of target organisms would greatly improve the
136 performance of indices.

137 Patch connectivity indices with appropriate scaling used in on patches with adequate
138 delineation can still yield limited effects on local species richness. This occurs for instance if
139 structural connectivity little fluctuates among patches or if immigration does not act as a
140 source of species diversity. Limited fluctuation in patch connectivity indices arises when most
141 patches have similar surrounding habitat availability. For a given quantity of habitat in a
142 landscape, we anticipated that the variance of surrounding habitat availability among patches
143 increased with habitat aggregation. Here, we therefore aimed at testing whether, habitat
144 amount being kept constant, a stronger aggregation of the habitat map would lead to
145 stronger fluctuation of patch connectivity indices, hence creating opportunities to observe
146 connectivity effects on local species richness.

147 Furthermore, even if patch structural connectivity adequately depicts immigration and varies
148 among patches, it can affect local species richness only if the immigrant pool coming to the
149 focal patch harbors a moderate-to-high species diversity. The immigrant pool is made of a
150 mixture of emigrants from patches in the surrounding landscape. Consequently, the diversity
151 of the immigrant pool is tightly linked to the concept of γ -diversity [15] of the surrounding
152 landscape (i.e. mixing all patches together). For a given amount of surrounding habitat
153 (controlled by patch connectivity indices), the gamma diversity of the surrounding landscape
154 depends on the spatial configuration of the habitat, although the relationship can be labile. If
155 the surrounding habitat has high landscape connectivity in the absence of the focal patch, it
156 may increase the local species diversity in each patch contributing to the immigrant pool (α -
157 diversity in the surrounding landscape; e.g. [16]). However, it may also decrease the
158 dissimilarity in species composition among contributing patches (β -diversity in the
159 surrounding landscape; e.g. [16]), resulting in uncertain global effect on the γ -diversity.
160 Nonetheless, a robust conclusion is that the spatial configuration of the surrounding habitat is
161 likely to generate “noise” on the patch connectivity – species richness relationship, and such
162 noise may contribute to weaken the explanatory power of patch connectivity indices on
163 species richness. Patch-based “connector” indices [17] can contribute to pinpoint fluctuation
164 in landscape connectivity around the focal patch. These indices capture to what extent the
165 focal patch contributes to the connection among the other patches in the landscape. For a
166 given amount of habitat around the focal patch, a lower connector score of the focal patch
167 therefore indicates that surrounding patches depend less on the focal patch to connect one
168 with another, i.e. that direct fluxes among surrounding patches are stronger. Here we aimed
169 at testing whether the explanatory power of patch connectivity indices on the local species

170 richness decreased when the connector status of sampled patches have strong independent
171 fluctuations, which we called “connector noise”. Because [18] showed that connector indices
172 are often decoupled from patch connectivity indices in space, this situation was likely to
173 occur in our simulations and in the real world, hence worth considering here.

174 In our analysis, we successively focused on how patch delineation, scaling of patch
175 connectivity indices, index type and landscape features (including variation of patch
176 connectivity index and connector noise) affect the explanatory power of patch structural
177 connectivity on local species richness. We used a virtual ecologist approach [19] relying on
178 metacommunity simulations in a spatially-explicit model. Virtual datasets stemming from
179 such models constituted an ideal context to assess the impact of our factors of interest, for
180 they offered perfect control of the spatial distribution of habitat and the ecological features of
181 species. In particular, they only included processes related to the TIB (immigration,
182 ecological drift; [20]), thus maximizing our ability to study how methodological choices and
183 landscape features affect the explanatory power of patch structural connectivity. We
184 anticipated that explanatory powers generated by this approach would necessarily be an
185 over-estimation of what occurs in real ecosystems, where many processes unrelated to TIB
186 may be at work. However, feedbacks from our virtual approach to real ecosystems readily
187 arise when considering that settings that negatively affects the explanatory power of patch
188 structural connectivity in our approach have very little chance to yield strong explanatory
189 power of patch structural connectivity on local species richness in empirical studies.

190 Materials and methods

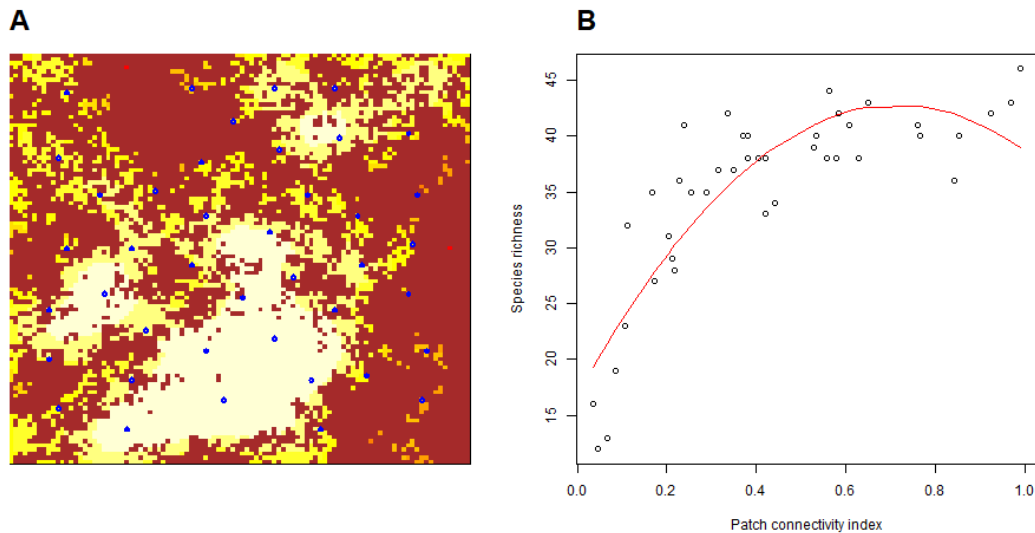
191 **Landscape generation** - We considered binary landscapes made of suitable habitat cells
192 and inhospitable matrix cells. We generated virtual landscapes composed of 100×100 cells
193 using a midpoint-displacement algorithm [21] which allowed us covering different levels of
194 habitat quantity and fragmentation. The proportion of habitat cells varied according to three
195 modalities (10%, 20% of 40% of the landscapes). The spatial aggregation of habitat cells
196 varied independently, and was controlled by the Hurst exponent (0.1, 0.5, and 0.9 in
197 increasing order of aggregation; see Fig. S1 for examples). Ten replicates for each of these
198 nine landscape types were generated, resulting in 90 landscapes. Higher values of the Hurst
199 exponent for a given value of habitat proportion increased the size of sets of contiguous cells
200 and decreased the number of distinct sets of contiguous cells (Fig. S2). Higher habitat
201 proportion for a constant Hurst coefficient value also resulted in higher mean size of sets of
202 contiguous cells.

203 Neutral metacommunity simulations - We simulated spatially explicit neutral
204 metacommunities on virtual heterogeneous landscapes. We resorted to using a spatially
205 explicit neutral model of metacommunities, where all species have the same dispersal
206 distance. We used a discrete-time model where the metacommunity changes by steps. All
207 habitat cells were occupied, and community dynamics in each habitat cell followed a zero-
208 sum game, so that habitat cells always harbored 100 individuals at the beginning of a step.
209 One step was made of two consecutive events. Event 1: 10% of individuals die in each cell –
210 they are picked at random. Event 2: dead individuals are replaced by the same number of
211 recruited individuals that are randomly drawn from a multinomial distribution, each species
212 having a weight equal to $0.01 \times \chi_i + \sum_k A_{ik} \exp(-d_{kf} / \lambda_s)$ where χ_i is the relative abundance of
213 species i in the regional pool, A_{ik} is the local abundance of species i in habitat cell k , d_{kf} is the
214 Euclidean distance (in cell unit) between the focal habitat cell f and the source habitat cell k ,
215 λ_s is a parameter defining species dispersal distances and the sum is over all habitat cells k
216 of the landscape. The regional pool was an infinite pool of migrants representing biodiversity
217 at larger spatial scales than the focal landscape, it contained 100 species, the relative
218 abundances of which were sampled once for all at the beginning of the simulation in a
219 Dirichlet distribution with concentration parameters α_i equal to 1 (with i from 1 to 100).
220 Metacommunity were simulated forward in time, with 1000 burn-in steps and 500 steps
221 between each replicates. Simulation was structured as a torus to remove unwanted border
222 effects in metacommunity dynamics. Metacommunities were simulated with three levels of
223 species dispersal $\lambda_s = 0.25, 0.5, 1$ cell, which corresponded to median dispersal distance of
224 0.6, 0.7, 0.9 cell and average dispersal distance of 0.6, 0.8, 1.2 cells. Because dispersal
225 distance distribution is skewed, it is also insightful to give the 95% quantile of dispersal
226 distance, which corresponded to 1.2, 1.7, 3.1 cells respectively, and shows the potential of
227 species in terms of long-distance dispersal. We performed 10 replicates for each dispersal
228 value and in each landscape. In total, we obtained of 3 Hurst coefficient values \times 3 habitat
229 proportion \times 3 species dispersal level \times 10 landscape replicates \times 10 community replicates =
230 2700 metacommunity simulations. For each metacommunity simulation, species richness
231 was computed at the cell level with R [22].

232 Finally, we built one virtual dataset per simulation. We considered communities in habitat
233 cells away from each other's for a minimal distance of 12 cells, to reduce spatial auto-
234 correlation (e.g. Fig. 1A). We also reduced potential landscape border effect (that could
235 decouple landscape indices and actual migrants received) by excluding cells near landscape
236 borders (to a distance inferior or equal to eight cells, equivalent to the longest buffer radius).
237 Each landscape counted in average 25 sampled cells (CI-95% = [23, 27]).

238

239 **Figure 1 – Example of analysis of the explanatory power of a patch connectivity index**
240 **in a virtual dataset.** Panel A: a virtual landscape obtained through midpoint displacement
241 algorithm, with controlled habitat proportion (here 0.4) and Hurst coefficient (here 0.1). Brown
242 cells stands for unhospitable matrix. Red to yellow cells denote habitat cells with increasing
243 patch connectivity indices (here a Buffer index with radius 8 cells). Sampled cells are
244 selected (blue circles) with minimal distance from border and among cells. We simulated
245 metacommunity dynamics in the whole landscape. At the end of simulation, species richness
246 is recorded in sampled cells. Panel B: the relationship between patch connectivity and
247 sampled cells is analysed using a quadratic model (red curve), and the R^2 of the model,
248 called R^2_{spec} , is recorded for future analyses. When not significant, the quadratic term is
249 dropped. The community dispersal in the simulation presented here is $\lambda_s = 1$ cell.



250

251 **Local connectivity indices** - We first computed patch connectivity indices using a raster
252 perspective for patch delineation, considering each habitat cell in the landscape as a patch.
253 We called this approach “fine” patch delineation below. In the context of our simulation, it is
254 the appropriate patch delineation to consider, since habitat cells correspond to communities
255 in the metacommunity model. We computed three contrasted types of patch connectivity
256 indices (Table 1) for each sampled cell of virtual datasets: *Buffer*, *dF* and *dIICflux*. *Buffer*
257 indices correspond to the proportion of area covered by habitat patches within circles of
258 different radius ($r_{buf} = 1, 2, 4, 5, 8$ cells) around the focal sampled patch. *dIICflux* and *dF* were
259 based on nodes corresponding to patches. Pairs of nodes were connected to each other by
260 links. Links' weights w_{ij} between cells i and j in the network decreased according to the
261 formula $\exp(-d_{ij}/\lambda_c)$, where d_{ij} is the Euclidean distances between cells i and j and λ_c is a scale
262 parameter [14,23]. λ_c may be interpreted as the hypothesized scale of dispersal distance of
263 target organisms in the landscape (which may differ from the “true” simulated scale of
264 dispersal distance, which is λ_s). We considered four scale parameter values ($\lambda_c = 0.25, 0.5, 1$
265 and 2 cells). *dF* quantified the sum of edges weights between the focal patch (i.e. the

266 sampled cell) and all the other patches (i.e. all the other habitat cells of the landscape).
 267 *dIIcflux* considered a binary graph, where each cell pair was considered either connected (1)
 268 or not (0) relatively to a minimal link weight $w_{\min} = 0.005$. Scale parameters $\lambda_c = 0.25, 0.5, 1$
 269 and 2 cells thus lead to connect all pairs of habitat cells separated by a distance inferior to
 270 1.3, 2.6, 5.3 and 10.6 cells respectively. In particular, binary graph for $\lambda_c = 0.25$ hence
 271 corresponded to the classic stepping-stone on a grid. *dIIcflux* captured a notion of node
 272 centrality, like *dF*, but based on topological distance in the graph rather than Euclidean
 273 distance. All indices were computed with Conefor 2.7 (command line version for Linux,
 274 furnished by S. Saura, soon publicly available on www.conefor.org; [24]).

275 **Table 1 — Patch connectivity indices considered in the study**

Index	Definition	Ref.
Buffer	$\text{buf}_k = \frac{a}{\pi r^2} \sum_{\substack{i=1 \\ i \neq k}}^n 1_{d_{ik} \leq r}$	[8]
dIIcflux	$\text{dIIcflux}_k = \frac{100}{IIc} \left[2 \sum_{\substack{i=1 \\ i \neq k}}^n \frac{a_k a_i}{1 + n_{ij}} \right]$	[17]
Flux	$\text{dF}_k = 2 \sum_{\substack{i=1 \\ i \neq k}}^n w_{ik}$	[14,23]

276 **Notations:** n : total number of nodes (patches or cells) in a graph; a : area of a cell; a_i : area of patch i ; r : radius of a buffer; n_{ij} :
 277 shortest path between nodes i and j in a binary graph; $IIc = \sum_{i=1}^n \sum_{j=1}^n a_i a_j / (1 + n_{ij})$: integral index of connectivity of a graph;
 278 d_{ij} : Euclidean distance between nodes i and j ; w_{ij} : probability weight of the link between nodes i and j in a weighted graph.

279 Then, we switched to a vector perspective in patch delineation, lumping together the groups
 280 of contiguous habitat cells in the map to form patches (Fig. S3), which we call a “coarse”
 281 patch delineation below. For each sampled cells, we computed the connectivity of the patch
 282 it belonged to. With this coarse patch delineation, patches contained several communities
 283 connected by limited dispersal. Altogether, we computed 28 distinct patch connectivity
 284 indices in each sampled cell of each simulation.

285 **General statistical approach** – We analyzed the explanatory power of patch connectivity
 286 indices on local species richness in simulated datasets. The explanatory power of a patch
 287 connectivity index on species richness is defined as the R^2 coefficient of the model *Species*
 288 *richness* ~ *Patch connectivity* + (*Patch connectivity*)², where we dropped the quadratic term
 289 when not significant (e.g. Fig. 1B). We denoted these R^2 coefficients as “ R^2_{spec} ” below. Most
 290 of our analyses consisted in analyzing how patch delineation, index scaling and landscape
 291 features affect R^2_{spec} , using linear models with R^2_{spec} as a dependent variable.

292 **Patch delineation** – We first considered *dF* and *dIIcflux* patch connectivity indices
 293 computed with a fine patch delineation. In each of the 2700 simulated dataset, we recorded

294 $R2_{spec}$ for dF or $dIICflux$. Both dF and $dIICflux$ had 4 possible scaling values, potentially
295 yielding four distinct $R2_{spec}$ values per index for the same virtual dataset. However, we only
296 kept the best value out of four in our analysis of patch delineation. We thus obtained 2'700
297 datasets \times 2 indices = 5'400 $R2_{spec}$ values.

298 Then we considered patch connectivity indices computed with a coarse patch delineation. In
299 each of the 2700 simulated dataset, we fitted a linear model with species richness as a
300 dependent variable. We used the connectivity index (dF or $dIICflux$) and the area of the patch
301 containing the sampled cell as independent variables. We included patch area in the analysis
302 to ensure fair comparison with the fine patch delineation analysis. Here again we included
303 quadratic terms (dF^2 or $dIICflux^2$, and $area^2$) when significant. We recorded $R2_{spec}$ of the
304 models and kept only the highest values across possible scaling parameters, which yielded
305 again $2'700 \times 2 = 5'400$ $R2_{spec}$ values.

306 We then analyzed the 10800 $R2_{spec}$ values generated above with one linear model per index
307 type (dF or $dIICflux$), where the dependent variable $R2_{spec}$ was modelled as a function of the
308 patch delineation ("coarse" or "fine") in interaction with landscape Hurst coefficient,
309 landscape habitat proportion and species dispersal distance (all these dependent variables
310 being considered as factors). We expected $R2_{spec}$ to be significantly higher at fine patch
311 delineation (despite the fact that area is included in the analysis at coarse patch delineation),
312 which we tested using the model $R2_{spec} \sim resolution$. We also expected the positive effect of
313 switching from coarse to fine resolution to increase when Hurst coefficient or habitat
314 proportion increase, because sets of contiguous cells become larger on average, leading to
315 stronger limited dispersal effects within patches. We tested this second hypothesis using two
316 models with interactions: $R2_{spec} \sim resolution \times Hurst\ coefficient$ and $R2_{spec} \sim resolution \times habitat$
317 $proportion$. At last, we expected the positive effect of switching from coarse to fine patch
318 delineation to decrease when species dispersal increases, because limited dispersal within
319 sets of contiguous cells weakens. We tested this last hypothesis using the model:
320 $R2_{spec} \sim resolution \times dispersal$.

321 **Index scaling** – We then considered $Buffer$, $dIICflux$ and dF patch connectivity indices
322 computed with a fine patch delineation. In each of the 2700 simulated dataset, we recorded
323 $R2_{spec}$ for each patch connectivity index and each scaling parameter value. We thus obtained
324 2'700 datasets \times 3 indices \times 4 or 5 scaling parameter values = 35'100 $R2_{spec}$ values. We then
325 built one linear model per index type ($Buffer$, dF or $dIICflux$), where $R2_{spec}$ was the dependent
326 variable, modelled as a function of species dispersal distance in interaction with index scale
327 parameter $R2_{spec} \sim dispersal \times scaling\ value$. We expected that the scale parameter yielding

328 the highest $R2_{spec}$ values increase with the dispersal distance of species, following previously
329 published results in the literature.

330 **Landscape features** – For each patch connectivity index type and each virtual dataset, we
331 considered a fine patch delineation and selected the scaling parameter value (within the
332 explored range) that maximized $R2_{spec}$. We recorded this maximal value of $R2_{spec}$, hence
333 generating 2700 virtual datasets \times 3 index types = 8100 R2 values.

334 We explored separately for each index at each species dispersal level how landscape
335 features (i.e. the habitat proportion and the Hurst coefficient) affected $R2_{spec}$ using the linear
336 model $R2 \sim Hurst\ coefficient \times habitat\ proportion$. We expected that landscapes the highest
337 Hurst coefficient value yield highest $R2_{spec}$.

338 We finally explored whether additional landscape features, beyond Hurst coefficient and
339 habitat proportion, could bring additional explanatory power on the variation of the $R2_{spec}$ with
340 optimal scaling and resolution among virtual datasets. We focused on Buffer index and
341 considered two additional landscape features.

342 For each of the 2700 virtual datasets, we computed the standard deviation of Buffer among
343 sampled cells (“Buffer s.d.”) and the explanatory power of Buffer over sampled cells’
344 connector value (“Connector R2”). We defined Connector R2 as the R^2 coefficient of the
345 model $connector\ value \sim Buffer + Buffer^2$. We used *dIICconnector* [17] as a connector value.
346 Like *dIICflux* presented above, *dIICconnector* is an index based on representing the habitat
347 map as a binary network of patch (recall that at fine resolution patches are cells). To obtain
348 the binary network, we used the same weighting procedure than for *dF* and *dIICflux*, and
349 chose a scaling parameter $\lambda_c = 2$ cells (the largest value considered in our study). We used
350 the same threshold on edges weight than above ($w_{min} = 0.005$) to decide whether patches
351 should be connected or not in the binary graph. We defined our two additional landscape
352 features of interest as the residual variation of *Buffer s.d.* and *Connector R2* with respect to
353 Hurst coefficient and habitat proportion. We computed them as the residuals of linear models
354 $Buffer\ s.d. \sim Hurst\ coefficient \times habitat\ proportion$ and $Connector\ R2 \sim Hurst\ coefficient \times$
355 $habitat\ proportion$ respectively (we applied one linear model per dispersal level).

356 For each species dispersal level, we fitted the model $R2_{spec} \sim Hurst\ coefficient \times habitat$
357 $proportion + residual\ Buffer\ s.d. + residual\ connector\ R2$ over the 900 virtual datasets. We
358 expected that *residual Buffer s.d.* have a significant positive effect on $R2_{spec}$. We also
359 predicted that *residual connector R2* have a significant positive effect on $R2_{spec}$. We
360 assessed the relative contribution of *Hurst coefficient \times habitat proportion*, *residual Buffer s.d.*
361 and *residual connector R2* using an analysis of variance.

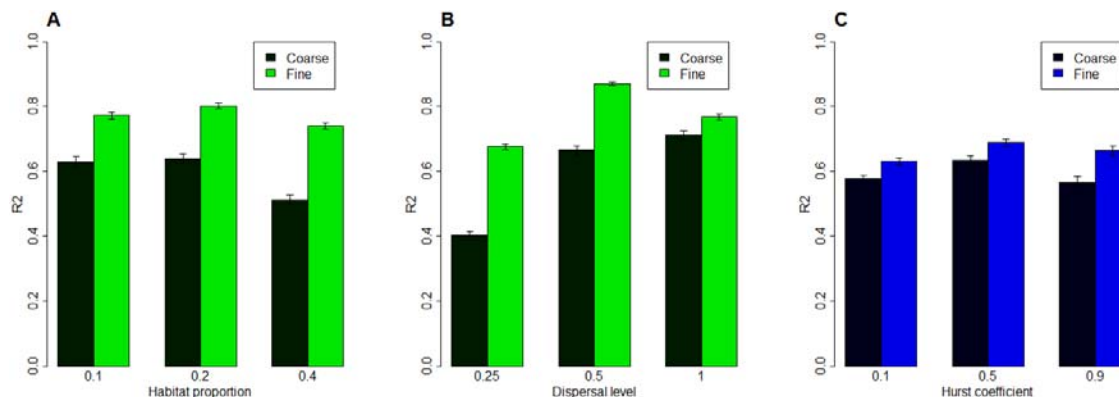
362 Results

363 Patch delineation – For both dF and $dIICflux$, using a fine patch delineation yielded higher
364 $R2_{spec}$ on average than using a coarse resolution (+0.18 with $p < 2e-16$ for dF ; +0.07 with
365 $p < 2e-16$ for $dIICflux$).

366 For dF index, the Hurst coefficient did not significantly affect the positive effect of refining
367 patch delineation on $R2_{spec}$. By contrast, a larger proportion of habitat in the landscape
368 increased the positive effect of refining patch delineation on $R2_{spec}$ (Fig. 2A): the effect of
369 refining patch delineation on $R2_{spec}$ reached +0.23 (estimate s.d. 0.01) for a habitat
370 proportion of 0.4 while it equaled +0.14 (estimate s.d. 0.01) only for a habitat proportion of
371 0.1. Higher species dispersal decreased the positive effect of refining patch delineation on
372 $R2_{spec}$ (Fig. 2B): the effect of refining patch delineation on $R2_{spec}$ reached +0.27 (estimate s.d.
373 0.01) when species had low dispersal abilities while it equaled +0.06 (estimate s.d. 0.01)
374 when species had high dispersal abilities.

375 For $dIICflux$ index, a higher Hurst coefficient increased the positive effect of refining patch
376 delineation on $R2_{spec}$ (Fig. 2C): the effect of refining patch delineation equaled +0.10
377 (estimate s.d. 0.01) in highly aggregated landscapes with a Hurst coefficient of 0.9 while the
378 effect of refining patch delineation equaled +0.05 only (estimate s.d. 0.01) in landscapes with
379 a Hurst coefficient of 0.1. Habitat proportion and species dispersal did not significantly affect
380 the effect of refining patch delineation on $R2_{spec}$.

381 **Figure 2 — Hurst coefficient, habitat proportion and species dispersal modulating the**
382 **effect of refining patch delineation on the explanatory power of patch connectivity**
383 **indices.** Bars show the average $R2_{spec}$ over simulated datasets for distinct levels of habitat
384 proportion (panel A), community dispersal (panel B) and Hurst coefficient (panel C), with
385 asymptotic 95% confidence intervals (half width = 1.96 x standard error). Panel A and B
386 come from the analysis of the dF index while Panel C comes from the analysis of $dIICflux$,
387 hence the different colors.



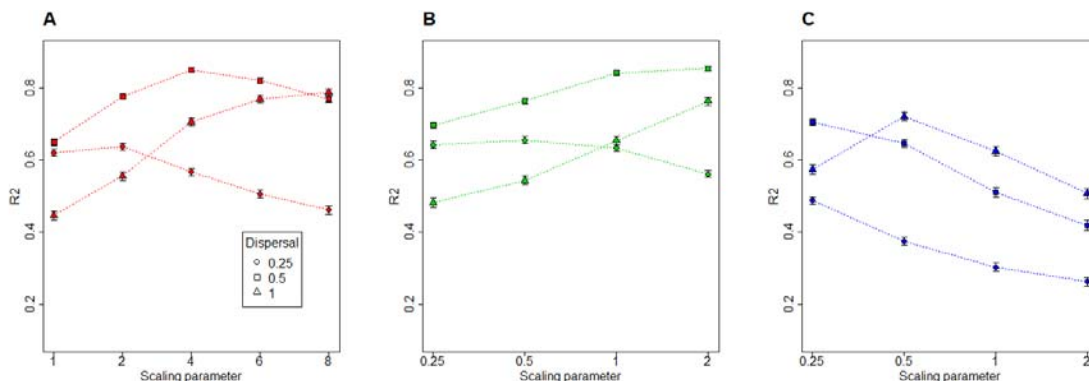
388

389 Index scaling and species dispersal –For *Buffer*, *dF* and *dIICflux*, the scaling parameter
390 value yielding the highest $R2_{spec}$ increased with species dispersal (Fig. 3).

391 For *Buffer* indices, the optimal scaling parameter value (i.e. *Buffer* radius r_{buf}) corresponded
392 to about 8 times the true scale of species dispersal (λ_s ; Fig. 3A). For *dF* indices, the optimal
393 scaling parameter (λ_c) corresponded to about 2 times the true scale of species dispersal (Fig.
394 3B). For *dIICflux* indices, the optimal scaling parameter (λ_c) rather corresponded to about 0.5
395 times the true scale of species dispersal (Fig. 3C; although the scope of scaling parameters
396 explored was not sufficient to ascertain this point for all the three dispersal levels explored).

397 For all species dispersal levels and all indices, $R2_{spec}$ varied broadly (by about 0.2) when
398 browsing possible scaling values. However, the optimal scaling value rarely yielded $R2_{spec}$
399 markedly different from those obtained from neighboring scaling values, except in some
400 specific cases where the optimal value lied at the boarder of the explored range (suggesting
401 that the true optimal scaling value is actually outside the explored range; see e.g. *dIICflux*
402 with species dispersal 0.25 on Fig. 3C).

403 **Figure 3 — Scaling parameter value effect on patch connectivity indices explanatory**
404 **power as a function of the scale of species dispersal.** Panels A, B and C correspond to
405 *Buffer*, *dF* and *dIICflux* indices respectively. Shapes correspond to the distinct community
406 dispersal levels tested in our analysis. The y-axis corresponds to the average R2 observed
407 across our virtual datasets for the target index when using the scaling parameter value
408 reported on the x-axis. Error bars correspond to asymptotic 95% confidence intervals (half
409 width = 1.96 x standard error).



410

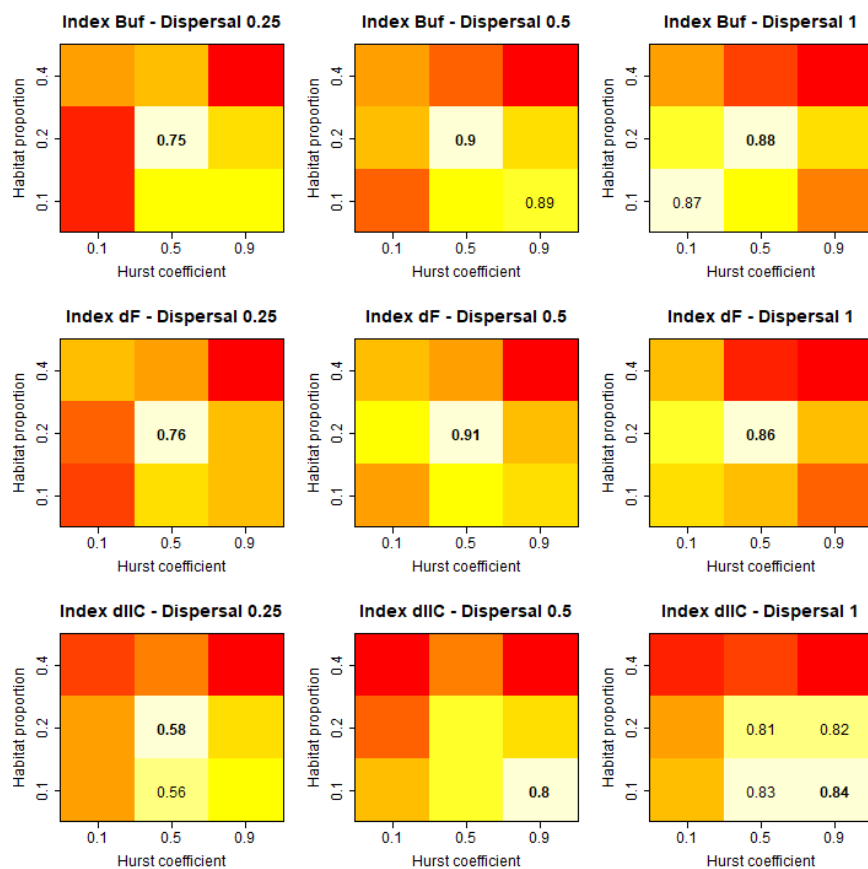
411

412 Global performance of indices - 95% of $R2_{spec}$ values at fine patch delineation with optimal
413 scaling lied between 0.30 and 0.96, with an average value of 0.74. *Buffer* and *dF* stood out
414 as the most performant index on average. The average $R2_{spec}$ of *Buffer* was $R2_{spec}=0.78$.
415 Average $R2_{spec}$ for *dF* index differed from *Buffer* by -0.01 only, which was a significant (z-test;

416 $p=0.03$) but very weak difference. By contrast, the average $R2_{spec}$ for *dIICflux* index differed
 417 from Buffer by -0.12 , which was a more significant (z-test; $p<2e-16$) and stronger difference.

418 Landscape effects - $R2_{spec}$ of patch connectivity indices were generally maximized for
 419 landscapes combining intermediary levels of the Hurst coefficient and intermediary levels of
 420 habitat proportion, irrespective of species dispersal (Fig. 4). The only exception occurred for
 421 *dIICflux* with medium or high species dispersal level, where landscapes with low habitat
 422 proportion and high aggregation yielded the highest $R2_{spec}$.

423 **Figure 4 — $R2_{spec}$ of patch connectivity indices as a function of landscape**
 424 **characteristics and dispersal level of species.** Each panel corresponds to one index type
 425 applied to virtual datasets with one species dispersal level (i.e. 900 virtual datasets).
 426 Columns correspond to dispersal levels (in cell unit), and lines to index type. Within a panel,
 427 average $R2_{spec}$ is reported for each combination of habitat proportion (y-axis) and Hurst
 428 coefficient (x-axis). Within a panel, the heat map shows the ordination of $R2_{spec}$ values with
 429 red corresponding to lowest values and white to highest ones. The maximum $R2_{spec}$ value is
 430 reported in bold letters, and all the other $R2_{spec}$ that are not significantly different from the
 431 maximum based on a z-test with threshold 5% are also reported.

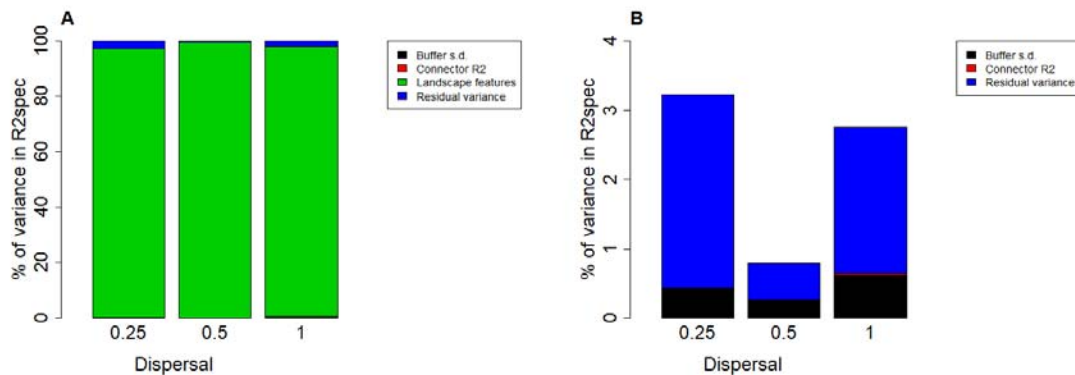


432

433 For *Buffer* index, the variation in Hurst coefficient and habitat proportion among virtual
 434 datasets explained between 97% and 99% of the variance in $R2_{spec}$ (Fig. 5). Residual *Buffer*
 435 *s. d.* had a significant positive on $R2_{spec}$, with standardized effect size (i.e. after scaling

436 residual *Buffer s. d.*) equal to 0.05 (estimate s.d. = 0.004), 0.05 (estimate s.d. = 0.002) and
437 0.06 (estimate s.d. = 0.004) for low, intermediate and high species dispersal respectively.
438 The effect of residual *Buffer s.d.* was therefore significant but consistently low and explained
439 a very limited amount of R^2_{spec} variance (around 0.5%; Fig. 5). The residual *Connector R2*
440 had a significant positive effect on R^2_{spec} at high species dispersal level only, but the
441 magnitude of the contribution was then negligible (Fig. 5).

442 **Figure 5 — Analysis of the variance in $Buffer R^2_{spec}$ among virtual datasets.** Variance is
443 decomposed into the contributions of: (i) the variation in landscape features (Hurst coefficient
444 in interaction with habitat proportion); (ii) the variation of *Buffer* standard deviation among
445 landscapes of similar features (“*Buffer s.d.*”); (iii) the variation in the explanatory power of
446 *Buffer* on the connector index in sampled cells among landscapes of similar features
447 (“*Connector R2*”). Contributions (y-axes) are expressed in percentages of the total variance
448 of R^2_{spec} . Panel A shows the whole decomposition. Panel B shows all the contributions
449 except that of landscape features, for better readability.



450

451 Discussion

452 **Patch delineation** – We have illustrated the problem of patch delineation in a binary design
453 comparing outputs of considering each elementary cell as a patch (the appropriate resolution
454 with respect to simulations) versus considering sets of contiguous cells as patches. Effects of
455 patch connectivity indices on local species richness were higher at fine patch delineation,
456 where no dispersal limitation occurred within patches. The coarser patch delineation
457 considering sets of contiguous habitat as patches led to important drop of explanatory power
458 in our results, reaching about -0.2 when species harbored strong dispersal limitation (Fig.
459 2B). In the light of our results, we therefore champion the “raster” perspective of [14]: even
460 when target habitats form “intuitive” patches (e.g. forest patches in agricultural landscapes),
461 one should define *a priori* a grid with appropriate mesh size, equal or lower to the scale of
462 dispersal for target organisms and use it to decompose the habitat map in elementary units.
463 We also insist on the fact that the raster perspective is perfectly compatible with the use of

464 graph theory concepts among cells, as we illustrated with the use of indices such as *dIICflux*
465 or *dIICconnector* on fine patch delineation.

466 Determining *a priori* the appropriate mesh size is not an easy task, especially since in real
467 communities – contrary to our simulations - movement capacity and dispersal are
468 heterogeneous among species. Beyond the binary comparison between coarse and fine
469 patch delineation that we proposed here, one should now explore the sensitivity of patch
470 connectivity indices explanatory power to varying mesh size (as suggested by [25] in real
471 empirical studies) This would allow assessing whether some degree of uncertainty on that
472 parameter is acceptable. We anticipate that using a too fine patch delineation should not lead
473 to heavy loss of explanatory power of patch connectivity indices on species richness, as long
474 as patch connectivity indices are rescaled appropriately. For instance, in our study design,
475 the range of probable dispersal distances (95% quantile) is closer to mesh size for low
476 species dispersal (1.2 cells) than for high species dispersal (3.1 cells). When species
477 dispersal is high, one could therefore argue that mesh size is unnecessarily small. However,
478 we did not observe important drops of power of patch connectivity indices when moving from
479 low to high species dispersal (e.g. Fig. 4). If using too fine a mesh size is harmless, mesh
480 size should thus be adjusted on the limiting species in terms of movement capacity in
481 communities with heterogeneous movement and dispersal, i.e. those that are the less mobile
482 in space and interact with other organisms only at fine scale. This approach should probably
483 be preferred to approaches based e.g. on the average movement capacity across species of
484 the community.

485 However, choosing very fine patch delineation can be computationally challenging, since it
486 can increase by several orders of magnitude the number of spatial units. This particularly
487 affect indices stemming from graph theory that needs to determine shortest paths between
488 all pairs of spatial units. Here we have been able to compute *dIICflux* and *dIICconnector*
489 indices in all the virtual landscapes at fine resolution (up to 4000 habitat units in a single
490 landscape). Consequently, indices based on binary networks seem to pass the test of
491 computational time. By contrast, we were unable to compute analogous indices in weighted
492 networks (*dPCflux* and *dPCconnector*, [26]).

493 **Index scaling** – The scaling of patch connectivity indices leading to maximal explanatory
494 power on species richness (the “scale of effect” sensu [11]) increased with the dispersal
495 distance of target organism, in line with previous findings on virtual studies [10,11]. This is a
496 strong argument to prefer patch connectivity indices with a scaling parameter that can be
497 modulated to match the dispersal ability of organisms rather than indices that cannot be
498 adapted like distance to nearest patch. It also confirms that the scale of effect should capture

499 some quantitative features of species dispersal, as it is often contended in the empirical
500 literature (e.g. [27,28]).

501 However, the scale of effect should not be used as a quantitative estimate of dispersal
502 distance for two reasons. First, we observed that scaling parameter values around the
503 optimal one often generated a very small loss of explanatory power, suggesting that the
504 explanatory power was not highly sensitive to errors on scaling parameter value. Therefore,
505 finding the scaling parameter that maximizes the correlation is probably not an accurate
506 method to obtain estimate of species dispersal level. This is consistent with the fact that, in
507 empirical systems, buffer radii maximizing the explanatory power over species presence or
508 abundance can spread over a large array of distances without significant drop of explanatory
509 power, sometimes covering several orders of magnitude (e.g. [29]). Second, the quantitative
510 relationship between the scale of effect and species dispersal was labile. We identified linear
511 relationships between the scale of effect and the scale of species dispersal used in
512 simulations (λ_s), but the slope was very different depending on the index used. In addition, no
513 analogous linear relationships arose when considering average, median or 95% quantile of
514 species dispersal, contrary to what was evidenced by [11] on abundance in a virtual
515 metapopulation study.

516 Therefore, the relationship between the scale of effect and the scale of species dispersal
517 distance can contribute to ranking dispersal distance among species or groups of species
518 with marked differences. It can also contribute, when some *a priori* information is available
519 about the dispersal distance of target organisms, to defining the range of scaling parameter
520 values in which the scale of effect should be searched for.

521 Here we considered neutral metacommunities where all the species have the same dispersal
522 distance. This greatly simplified the analysis of the relationship between the scale of effect of
523 indices and species dispersal distances. However, species dispersal distances in real
524 communities are known to be heterogeneous [30,31], as polymorphism on dispersal is a
525 strong driver of species coexistence at metacommunity scale [32,33]. One may therefore
526 question how our findings can transfer to real empirical studies. We already commented
527 earlier that for a given species dispersal distance a quite broad range of scaling parameters
528 for a given index can lead to levels of explanatory power similar to that of the scale of effect.
529 While we presented this pattern as an obstacle to species dispersal estimation, it could turn
530 out to be an advantage when species have heterogeneous species dispersal strategy. As a
531 matter of fact, a scaling parameter value adapted to the average dispersal distance of
532 species in the community might be fairly adapted to all the species in the community. Of

533 course, this should not be valid anymore if species dispersal is highly heterogeneous among
534 species.

535 **Global performance of indices** – Indices used with appropriate scaling and fine spatial
536 resolution yielded very high explanatory power values on species richness, way above what
537 usually occurs in empirical studies. We expected that result, which stems from the fact that
538 our simulations only include processes compatible TIB, i.e. limited dispersal and ecological
539 drift, and force species dispersal to be equal. By doing so, it creates ideal conditions for high
540 explanatory power of patch connectivity on species richness to occur and offers us
541 magnifying glasses to focus on how patch delineation, indices properties and landscape
542 features can modulate it. Any downward effects on the explanatory power in our approach
543 could result in a total disappearance of patch connectivity explanatory power in real studies,
544 and should therefore be interpreted as bad conditions to study patch connectivity contribution
545 in empirical systems.

546 *Buffer* and *dF* indices lead to high and very similar performance when used with appropriate
547 scaling. This stemmed from the fact that these two indices are highly correlated (average
548 correlation across landscapes above 0.95; Figure S4). In our study, *Buffer* resembled *dF*
549 index when the buffer radius was about 4 times the *dF* scaling parameter value. [8] had
550 already evidenced that correlations between IFM index (a generalization of the *dF* index;
551 [34]) and buffers could reach 0.9 in a real landscape (their study did not focus on how the
552 scaling of both indices could affect the correlation). Such a similarity between *Buffer* and *dF*
553 on patches with fine delineation was quite expected since both indices share the same
554 general structure: a weighted sum of surrounding habitat cells contribution where weights
555 decreases with Euclidean distance following some kernel function. Regarding the shape of
556 the kernel, *Buffer* is based on a step function while *dF* is based on an decreasing exponential
557 kernel. We therefore interpret our results as the fact that changing the decreasing function
558 used as a kernel may little affect the local connectivity as long as scaling is adjusted. This
559 may explain why [5] found that: (i) switching from buffer to continuously decreasing kernel
560 little affected AIC or pseudo- R^2 of models used to predict species abundances; (ii) neither
561 continuously decreasing nor step function was uniformly better to explain species abundance
562 across four case studies; (iii) different continuous shapes of kernel had quite indiscernible
563 predictive performance.

564 The *dIICflux* index had a lower explanatory power than *Buffer* and *dF* indices on average (-
565 0.12 on R_{spec}). This difference in global performance was made possible by the fact that
566 *dIICflux* harbored a different profile than *dF* and *Buffer* in landscapes (Fig. S4), because it
567 considers topological rather than Euclidean distance to compute connectivity. The use of five

568 scaling values only in our analysis calls for some caution in the interpretation *dIICflux* lower
569 explanatory power. The optimal scaling value of *dIICflux* for low and intermediate dispersal
570 seemed to lie below the lower limit of the range explored in our study. Consequently the
571 explanatory power of this index might be underestimated compared to the other ones and
572 partly explain why it seems less efficient in predicting species richness.

573 Part of the relative success of *dF* and *Buffer* over *dIICflux* may also stem from the fact that
574 we did not include different resistance values to habitat and matrix cells. When
575 heterogeneous resistance occurs, landscape connectivity including displacement costs (e.g.
576 least cost path, circuit theory) can be markedly different from prediction based on Euclidean
577 distance only [35], and may better capture the movement of organisms in real case study
578 [36,37]. This probably also applies to patch connectivity. By connecting only cells that contain
579 habitat, *dIICflux* and other indices based on topological distance within a graph could prove
580 more performant when matrix has high resistance cost, and we may not find the same
581 superiority of Euclidean indices as in our simulations. However, some of our results here
582 should remain true when resistance is heterogeneous in space, at least qualitatively. Indeed,
583 since our study is purely virtual, we could as well consider that distances among cells in the
584 habitat map are not Euclidean but ecological distances. This would have amounted to saying
585 that landscapes considered in our study are “distorted” maps compared to reality. Based on
586 this mind experiment, we would still expect that the optimal scaling of indices, expressed in
587 ecological distance, would increase with species dispersal, expressed in ecological distance
588 too. We also expect that our conclusion about the adequate delineation of patches should
589 also hold, but the mesh size in the real map should then fluctuate in space depending on the
590 resistance cost, shrinking in habitat areas with high resistance and expanding in habitat
591 areas with low resistance cost.

592 **Landscape effects** - Landscapes combining intermediary levels of the Hurst coefficient and
593 intermediary levels of habitat proportion yielded highest explanatory of *dF* and *Buffer* indices
594 used with adapted scaling at fine spatial resolution. We understood the unpredicted unimodal
595 effect of habitat proportion on the explanatory power as follows: high connectivity is unlikely
596 in landscapes with a very low amount of habitats while low connectivity is unlikely in
597 landscapes with a very low amount of habitats. As a result, the maximal range of variation in
598 patch connectivity lies in intermediary landscapes in terms of habitat proportion (Figure S5).
599 Our findings are reminiscent of the conceptual model of [38], which promoted the idea that
600 habitat spatial configuration should affect species abundance or persistence only in when
601 habitat amount lies in a intermediary range of values. The latter range is comprised between
602 a lower limit where the species cannot maintain in the landscape whatever the spatial
603 configuration and an upper limit where the species can maintain in the landscape whatever

604 the spatial configuration. Whether and how the levels of habitat proportion at which, one the
605 one hand, patch connectivity – local species richness relationship arises and, on the other
606 hand, species persistence is sensitive to landscape-scale configuration overlap is an open
607 question of practical interest. In particular, one may ask whether the presence of a patch
608 connectivity – local species richness could indicate that the habitat amount at landscape
609 scale has entered the intermediary range where considering the spatial configuration in
610 management plans becomes critical.

611 Contrary to what we predicted, the Hurst coefficient had a modal effect on the explanatory
612 power of dF and *Buffer* on species richness. The increasing part of the relationship actually
613 followed the predicted behavior: low aggregation creates landscapes where the habitat is
614 homogeneously spread in space, leading to low variance in patch connectivity among
615 sampled cells (Fig. S5), hence low explanatory power on species richness. Landscape with
616 high aggregations contained few distinct sets of large contiguous cells (Fig. S1, S2). The
617 variance in patch-connectivity of cells thus depended on the ratio between the distance to the
618 border of these sets and the scaling parameter of the patch connectivity index. When
619 dispersal was low, variation in patch connectivity could occur only in a thin stripe along the
620 border of the sets of contiguous cells, the rest of cells harboring a uniformly high, saturating
621 connectivity. There was therefore little opportunity for low connectivity, hence creating low
622 variance of patch connectivity indices (Fig. S5) leading to low explanatory value of indices on
623 species richness (Fig. 4). By contrast, when dispersal is medium or high, there was a
624 smoother contrast between border and interior of patches in term of connectivity, yielding
625 more opportunity for variance in patch connectivity and no negative effect of Hurst coefficient
626 on patch connectivity variance (Fig. S5). However, the effect size *Buffer* indices on species
627 richness still became smaller when switching from medium to high Hurst coefficient because
628 the average value of *Buffer* index increased and the variation in *Buffer* then fell within a
629 range of values where the corresponding species richness tended to saturate at an upper
630 threshold (Fig. S6). Given the tight level of correlation between *Buffer* and dF , our
631 conclusions about *Buffer* can be harmlessly transferred to dF index.

632 The variance in *Buffer* index among landscapes with identical Hurst coefficient and habitat
633 proportion had an additional positive effect on its explanatory power, as expected, but this
634 effect was clearly negligible compared to landscape influence. We had the same type of
635 conclusion regarding the potential perturbation induced by fluctuation in the connector status
636 of patches independently from their connectivity. We only detected a weak negative effect of
637 connector noise (the contrary of Connector R2) on the explanatory power of patch
638 connectivity indices at high species dispersal.

639 Conclusion

640 Our results suggest that finding a strong effect of patch structural connectivity on local
641 species richness can occur only if: (i) spatial units used as patches are sufficiently small to
642 prevent internal dispersal limitation within patches, which can be obtained by using a raster
643 perspective with appropriate mesh size for patch delineation; (ii) the scaling of the patch
644 connectivity index is adapted to the dispersal ability of species considered, which can be
645 obtained by browsing scaling parameters over a range of values defined from a priori
646 knowledge about species dispersal distance; (iii) the studied landscape shows intermediate
647 habitat amount and intermediate habitat fragmentation, so that the patch connectivity index
648 can harbor high variance among sampled patches. Notwithstanding the success of Buffer in
649 our approach, we suggest that similar analyses as ours should be performed with
650 heterogeneous resistance cost before recommending kernel-based indices using Euclidean
651 distance upon other choices. To date, point (iii) seems less straightforward to use in
652 empirical studies because it is not clear a priori what should be an “intermediate” habitat
653 amount or fragmentation and a “sufficient” level of variance in patch connectivity index for
654 some target set of species. It probably depends on species dispersal but maybe also on the
655 spatial extent of the study. Further work, dedicated to this point, is now needed in order to
656 define a full set of empirically verifiable conditions necessary for observing connectivity
657 effects on local species richness.

658 Acknowledgments

659 We thank Santiago Saura for sharing CONEFOR code. This work was part of the Patrames
660 project funded by the convention 2016 n°2101870336 of the French Ministry of Environment
661 (Water and Biodiversity Direction).

662 Conflict of interest disclosure

663 The authors of this preprint declare that they have no financial conflict of interest with the
664 content of this article. FL and FJ belong to the panel of PCI Ecology recommenders.

665 References

- 666 1. MacArthur RH, Wilson EO. 1967 *The theory of island biogeography*. Princeton University Press.
667 Princeton, NJ.
- 668 2. Itescu Y. 2019 Are island-like systems biologically similar to islands? A review of the evidence.
669 *Ecography* **42**, 1298–1314. (doi:10.1111/ecog.03951)

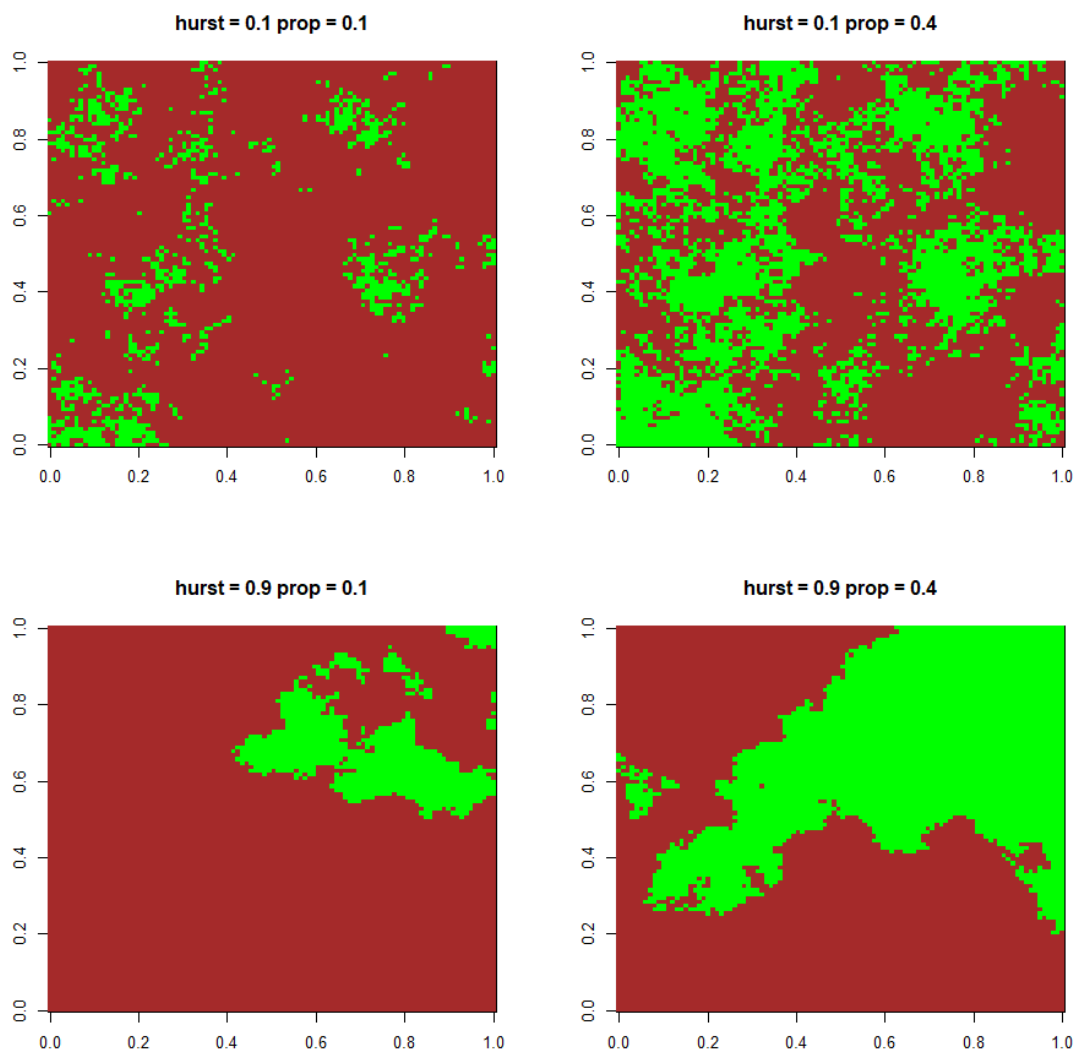
- 670 3. Haila Y. 2002 A conceptual genealogy of fragmentation research: from island biogeography to
671 landscape ecology. *Ecological Applications* **12**, 321–334. (doi:10.1890/1051-
672 0761(2002)012[0321:ACGOFR]2.0.CO;2)
- 673 4. Tischendorf L, Fahrig L. 2001 On the use of connectivity measures in spatial ecology. A reply.
674 *Oikos* **95**, 152–155. (doi:10.1034/j.1600-0706.2001.950117.x)
- 675 5. Miguet P, Fahrig L, Lavigne C. 2017 How to quantify a distance-dependent landscape effect on a
676 biological response. *Methods in Ecology and Evolution* **8**, 1717–1724. (doi:10.1111/2041-
677 210X.12830)
- 678 6. Prugh LR, Hodges KE, Sinclair ARE, Brashares JS. 2008 Effect of habitat area and isolation on
679 fragmented animal populations. *Proc Natl Acad Sci USA* **105**, 20770.
680 (doi:10.1073/pnas.0806080105)
- 681 7. Thornton DH, Branch LC, Sunquist ME. 2011 The influence of landscape, patch, and within-
682 patch factors on species presence and abundance: a review of focal patch studies. *Landscape*
683 *Ecology* **26**, 7–18. (doi:10.1007/s10980-010-9549-z)
- 684 8. Moilanen A, Nieminen M. 2002 Simple connectivity measures in spatial ecology. *Ecology* **83**,
685 1131–1145. (doi:10.1890/0012-9658(2002)083[1131:SCMISE]2.0.CO;2)
- 686 9. Vieira MV, Almeida-Gomes M, Delciellos AC, Cerqueira R, Crouzeilles R. 2018 Fair tests of the
687 habitat amount hypothesis require appropriate metrics of patch isolation: An example with small
688 mammals in the Brazilian Atlantic Forest. *Biological Conservation* **226**, 264–270.
689 (doi:10.1016/j.biocon.2018.08.008)
- 690 10. Economo EP, Keitt TH. 2010 Network isolation and local diversity in neutral metacommunities.
691 *Oikos* **119**, 1355–1363.
- 692 11. Jackson HB, Fahrig L. 2012 What size is a biologically relevant landscape? *Landscape Ecology*
693 **27**, 929–941. (doi:10.1007/s10980-012-9757-9)
- 694 12. Kotliar NB, Wiens JA. 1990 Multiple Scales of Patchiness and Patch Structure: A Hierarchical
695 Framework for the Study of Heterogeneity. *Oikos* **59**, 253–260. (doi:10.2307/3545542)
- 696 13. Gascuel F, Laroche F, Bonnet-Lebrun A-S, Rodrigues ASL. 2016 The effects of archipelago
697 spatial structure on island diversity and endemism: predictions from a spatially-structured neutral
698 model. *Evolution* **70**, 2657–2666. (doi:10.1111/evo.13067)
- 699 14. Urban D, Keitt T. 2001 Landscape connectivity: a graph-theoretic perspective. *Ecology* **82**, 1205–
700 1218. (doi:10.1890/0012-9658(2001)082[1205:LCAGTP]2.0.CO;2)
- 701 15. Whittaker RH. 1972 Evolution and measurement of species diversity. *Taxon* **21**, 213–251.
- 702 16. Economo EP, Keitt TH. 2008 Species diversity in neutral metacommunities: a network approach.
703 *Ecology Letters* **11**, 52–62.
- 704 17. Saura S, Rubio L. 2010 A common currency for the different ways in which patches and links can
705 contribute to habitat availability and connectivity in the landscape. *Ecography* **33**, 523–537.
706 (doi:10.1111/j.1600-0587.2009.05760.x)
- 707 18. Baranyi G, Saura S, Podani J, Jordán F. 2011 Contribution of habitat patches to network
708 connectivity: Redundancy and uniqueness of topological indices. *Ecological Indicators* **11**, 1301–
709 1310. (doi:10.1016/j.ecolind.2011.02.003)

- 710 19. Zurell D *et al.* 2010 The virtual ecologist approach: simulating data and observers. *Oikos* **119**,
711 622–635. (doi:10.1111/j.1600-0706.2009.18284.x)
- 712 20. Hubbell SP. 2001 *The unified neutral theory of biodiversity and biogeography*. Princeton, NJ:
713 Princeton University Press.
- 714 21. Etherington TR, Holland EP, O’Sullivan D. 2015 NLMpy: a python software package for the
715 creation of neutral landscape models within a general numerical framework. *Methods in Ecology*
716 *and Evolution* **6**, 164–168. (doi:10.1111/2041-210X.12308)
- 717 22. R Core Team. 2016 *R: A language and environment for statistical computing*. Vienna, Austria: R
718 Foundation for Statistical Computing. See <https://www.R-project.org>.
- 719 23. Bunn AG, Urban DL, Keitt TH. 2000 Landscape connectivity: A conservation application of
720 graph theory. *Journal of Environmental Management* **59**, 265–278. (doi:10.1006/jema.2000.0373)
- 721 24. Saura S, Torné J. 2009 Conefor Sensinode 2.2: A software package for quantifying the importance
722 of habitat patches for landscape connectivity. *Environmental Modelling & Software* **24**, 135–139.
723 (doi:10.1016/j.envsoft.2008.05.005)
- 724 25. Mazerolle MJ, Villard M-A. 1999 Patch characteristics and landscape context as predictors of
725 species presence and abundance: A review1. *Écoscience* **6**, 117–124.
726 (doi:10.1080/11956860.1999.11952204)
- 727 26. Saura S, Pascual-Hortal L. 2007 A new habitat availability index to integrate connectivity in
728 landscape conservation planning: Comparison with existing indices and application to a case
729 study. *Landscape and Urban Planning* **83**, 91–103. (doi:10.1016/j.landurbplan.2007.03.005)
- 730 27. Ranius T. 2006 Measuring the dispersal of saproxylic insects: a key characteristic for their
731 conservation. *Population Ecology* **48**, 177–188.
- 732 28. Ranius T, Johansson V, Fahrig L. 2011 Predicting spatial occurrence of beetles and
733 pseudoscorpions in hollow oaks in southeastern Sweden. *Biodiversity and Conservation* **20**, 2027–
734 2040. (doi:10.1007/s10531-011-0072-6)
- 735 29. Bergman K-O, Jansson N, Claesson K, Palmer MW, Milberg P. 2012 How much and at what
736 scale? Multiscale analyses as decision support for conservation of saproxylic oak beetles. *Forest*
737 *Ecology and Management* **265**, 133–141. (doi:10.1016/j.foreco.2011.10.030)
- 738 30. Muller-Landau HC, Wright SJ, Calderón O, Condit R, Hubbell SP. 2008 Interspecific variation in
739 primary seed dispersal in a tropical forest. *Journal of Ecology* **96**, 653–667. (doi:10.1111/j.1365-
740 2745.2008.01399.x)
- 741 31. Cadotte MW, Mai DV, Jantz S, Collins MD, Keele M, Drake JA. 2006 On Testing the
742 Competition–Colonization Trade–Off in a Multispecies Assemblage. *The American Naturalist*
743 **168**, 704–709. (doi:10.1086/508296)
- 744 32. Calcagno V, Mouquet N, Jarne P, David P. 2006 Coexistence in a metacommunity: the
745 competition–colonization trade–off is not dead. *Ecology Letters* **9**, 897–907.
- 746 33. Laroche F, Jarne P, Perrot T, Massol F. 2016 The evolution of the competition–dispersal trade-off
747 affects α - and β -diversity in a heterogeneous metacommunity. *Proceedings of the Royal Society of*
748 *London B: Biological Sciences* **283**. (doi:10.1098/rspb.2016.0548)
- 749 34. Hanski I. 1994 A practical model of metapopulation dynamics. *Journal of Animal Ecology* **63**,
750 151–162. (doi:10.2307/5591)

- 751 35. Simpkins CE, Dennis TE, Etherington TR, Perry GLW. 2018 Assessing the performance of
752 common landscape connectivity metrics using a virtual ecologist approach. *Ecological Modelling*
753 **367**, 13–23. (doi:10.1016/j.ecolmodel.2017.11.001)
- 754 36. Emel SL, Storfer A. 2015 Landscape genetics and genetic structure of the southern torrent
755 salamander, *Rhyacotriton variegatus*. *Conservation Genetics* **16**, 209–221. (doi:10.1007/s10592-
756 014-0653-5)
- 757 37. Vuilleumier S, Fontanillas P. 2007 Landscape structure affects dispersal in the greater white-
758 toothed shrew: Inference between genetic and simulated ecological distances. *Ecological*
759 *Modelling* **201**, 369–376. (doi:10.1016/j.ecolmodel.2006.10.002)
- 760 38. Villard M-A, Metzger JP. 2014 REVIEW: Beyond the fragmentation debate: a conceptual model
761 to predict when habitat configuration really matters. *Journal of Applied Ecology* **51**, 309–318.
762 (doi:10.1111/1365-2664.12190)
- 763

764 Supplementary figures

765 **Figure S1: Four examples of extreme landscapes in terms of aggregation (hurst) and**
766 **habitat proportion (prop) in our study. Habitat is pictured in green, matrix in brown.**

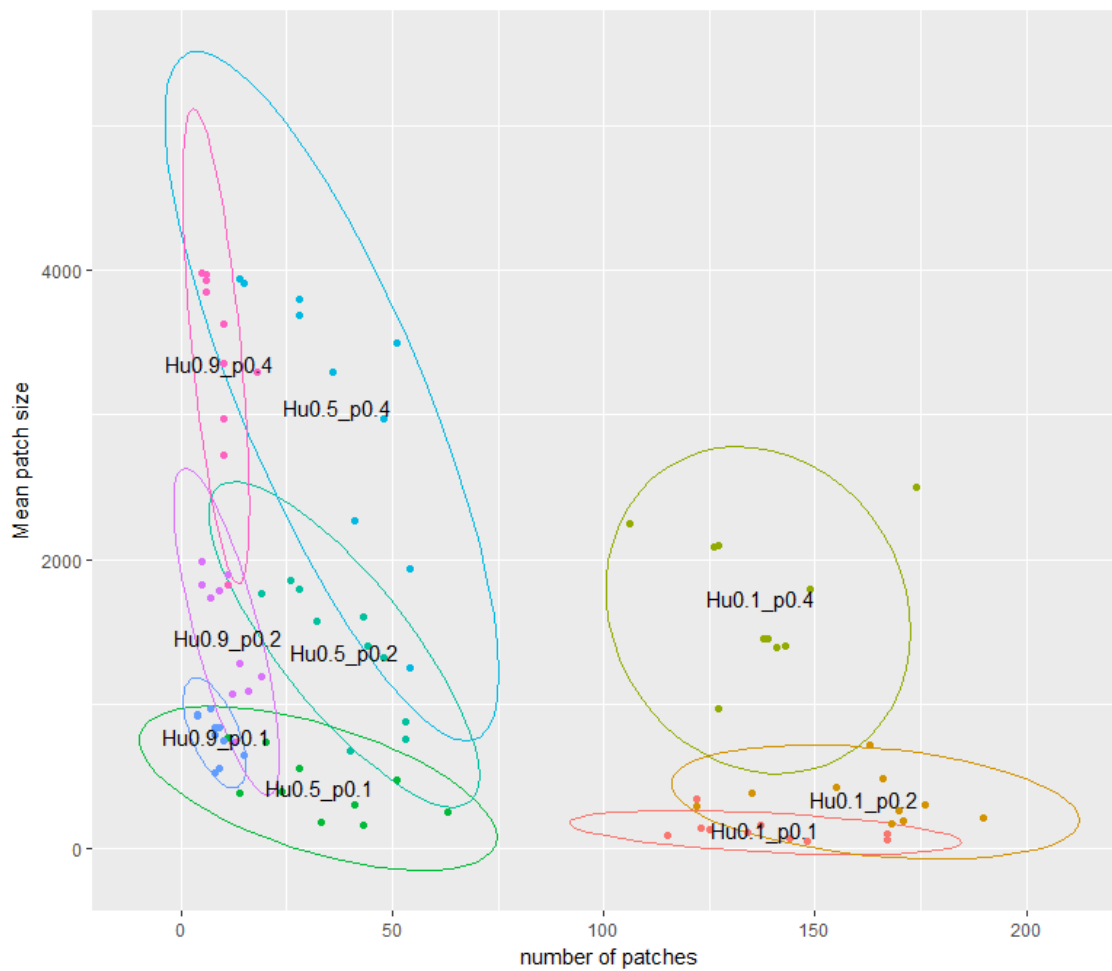


767

768

769 **Figure S2: Average size and number of patches in the virtual landscapes used in our**
770 **study.** Colors correspond to distinct combinations of Hurst exponent and habitat proportion.
771 Ellipses correspond to 95%-CI of a fitted bivariate Student distribution.

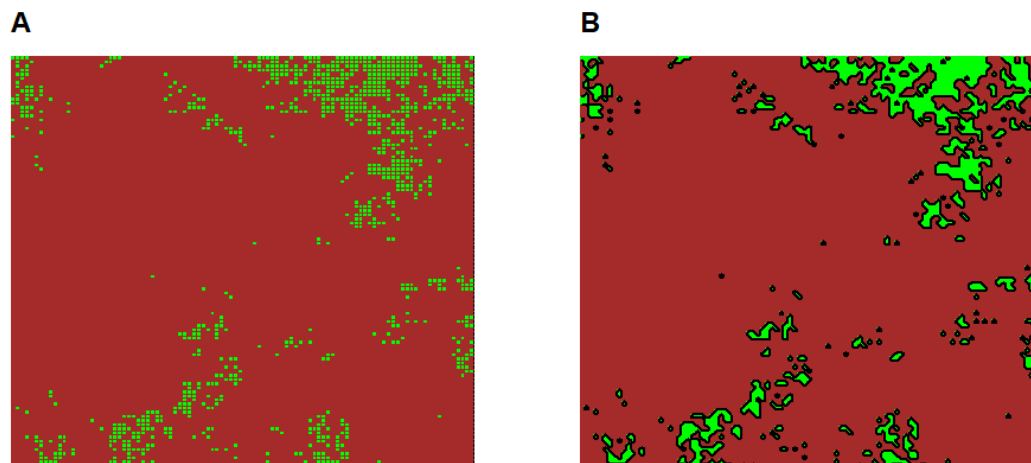
772



773

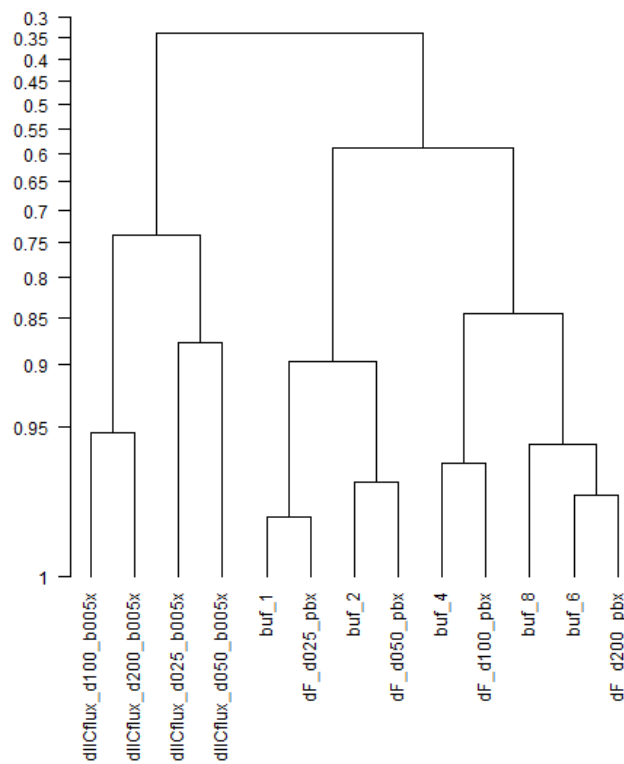
774

775 **Figure S3: Lumping of contiguous cells generating the coarse patch delineation**
776 **perspective.** Panel A shows a habitat map where fine delineation of patches has been
777 applied. Panel B shows the same habitat map where coarse patch delineation has been
778 applied, i.e. sets of contiguous cells has been lumped together. Contiguity is based on the
779 Von Neuman neighborhood of cells.



780

781 **Figure S4: Dendrogram of Pearson correlation coefficients among patch structural**
 782 **connectivity indices across all landscapes.** We presented correlations among *Buffer*, *dF*
 783 and *dIICflux* using ascending hierarchical classification. Within each of the 90 simulated
 784 landscapes, we computed the values of the 13 indices (accounting for distinct scaling values)
 785 in all habitat cells, which yielded 13 vectors of length 1000 to 4000 depending on the habitat
 786 proportion. We scaled each of the 13 vectors to mean 0 and variance 1, divided them by the
 787 square root of the number of habitat cells in the landscapes and computed pairwise
 788 Euclidean distances among them. We thus obtained one 13×13 distance matrix among patch
 789 connectivity indices in each of the 90 landscapes. Note that the distance between two indices
 790 corresponds to $\sqrt{2 - 2r}$, where r is the Pearson correlation between the indices across all
 791 habitat cells of the considered landscapes. We then averaged the 90 distance matrices to
 792 obtain one single 13×13 distance matrix as a basis for classification. We ran an ascending
 793 non-supervised classification (*hclust* function of R *base* package), using the *complete*
 794 method for group merging. A monophyletic group G with common ancestor located at value r
 795 means that any pair of indices within G has a correlation above r . Indices labels in the
 796 dendrogram are made of three parts separated by underscores “_”. The first part of the name
 797 indicates the type of the index (“buf”, “dF”, “dIICflux”). The second part of the name indicates
 798 the scale parameter of the index (“d025”, “d050”, “d100”, “d200” corresponding to $\lambda_c = 0.25$,
 799 0.5, 1, 2 cells respectively, and “1”, “2”, “4”, “6”, “8” corresponding to buffer radius r_{buf}
 800 in cells). The last part in meaningless here.



Structural connectivity indices

Figure S5: Standard deviation of *Buffer* with optimal scaling as a function of landscape characteristics and dispersal level of species. Each panel corresponds to one species dispersal level (i.e. 900 virtual datasets). Within a panel, average standard deviation of *Buffer* index among sampled cells is reported for each combination of habitat proportion (y-axis) and Hurst coefficient (x-axis). Within a panel, the heat map shows the ordination of standard deviation values with red corresponding to lowest values and white to highest ones. The maximum average standard deviation value is reported in bold letters, and all the other values that are not significantly different from the maximum based on a z-test with threshold 5% are also reported.

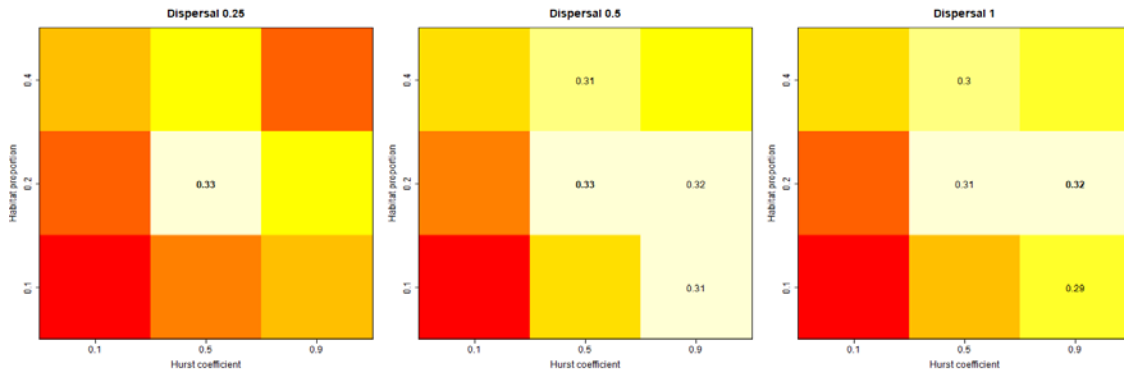


Figure S6: *Buffer* response to high landscape Hurst coefficient. In all panels, the species dispersal is $\lambda_s=1$, the highest value explored in our study. *Buffer* index has a radius $r_{buf}=8$ cells which is the optimal scaling given λ_s . Left panel: an example of fit of the model $species\ richness \sim Buffer + Buffer^2$ for intermediary habitat proportion and intermediary Hurst coefficient. The coefficient of determination R_{spec} is reported in bold. Center panel: an example of fit of the model $species\ richness \sim Buffer + Buffer^2$ for intermediary habitat proportion and high Hurst coefficient. The coefficient of determination R_{spec} is reported in bold. Right panel: boxplot of average *Buffer* value across sampled cells as a function of Hurst coefficient. The thick horizontal line shows the median value, boxes delimit first and third quantiles, and whiskers encompass all the data.

